Taylor & Francis
Taylor & Francis Group

Topological and geometrical disorders correlate robustly in two-dimensional foams

C. Quilliet[a]*, S. Ataei Talebi[a], D. Rabaud[a], J. Käfer[a], S.J. Cox[b] and F. Graner[a]

[a]*Laboratoire de Spectrométrie Physique, UMR5588, CNRS-Université Grenoble I, Martin d'Hères, France;* [b]*Institute of Mathematics and Physics, Aberystwyth University, Ceredigion, UK*

A two-dimensional (2D) foam can be characterised by its distributions of bubble area and number of sides. Both distributions have an average and a width (standard deviation). There are therefore at least two very different ways to characterise the disorder. The former is a geometrical measurement, while the latter is purely topological. We discuss the common points and differences between both quantities. We measure them in a foam which is sheared, so that bubbles move past each other and the foam is 'shuffled' (a notion we discuss). Both quantities are strongly correlated; in this case (only) it thus becomes sufficient to use either one or the other to characterise the foam disorder. We suggest applications in the analysis of other systems.

Keywords: foam; two dimensions; topology; geometry; disorder; shear

1. Introduction

Two-dimensional (2D) cellular patterns fill the plane without gaps or overlaps. Even if we consider here only the class of patterns where most cells meet in threes, they are ubiquitous in nature: from 2D foams to biological tissues, including geology, hydrodynamics, ecology and geography, as well as 2D cuts of three-dimensional foams and other cellular patterns in metallurgy, astronomy and biological organisms [1,2]. Each cell is characterised by its area A, which is an intrinsic property determined by the amount of matter it encloses, and its number of neighbours n, which can vary according to the mutual arrangement of cells within the pattern.

There are at least two quantities which characterise the disorder of a pattern: the distribution of A and the distribution of n [1–3]. In the present article, we study whether it is possible to simplify the description of disorder to only two numbers, namely the width of each distribution, called the geometrical and topological disorders, respectively. Both measures of disorder are independent [4,5].[1] However, statistically, a cell's value of n tends to increase with its size (perimeter or area): small cells tend to have fewer neighbours, and larger cells have more neighbours (see [1,2,6–14] and references therein). We can thus expect that, except when the initial conditions due to preparation are important, there is a correlation between these two measures of disorder.

---

*Corresponding author. Email: catherine.quilliet@ujf-grenoble.fr

We investigate here whether this intuition is correct and under which conditions the disorder of a pattern can statistically be described by a *single* number. We first describe experiments on a sheared monolayer of bubbles (Section 2), and compare the results (Section 3) with simulations of similar systems (Section 4).

2. Materials and methods

2.1. *Foam preparation*

The set-up is similar to that of Abd el Kader and Earnshaw [15]. We use a bubble monolayer (quasi-2D foam) confined at the air–water interface by a glass plate (Figure 1a), as introduced by Smith [7] and adapted by Vaz and Fortes [16]. It provides all the properties that we require (unlike both other quasi-2D foams, namely, those confined between two parallel glass plates or a bubble raft exposed to the air [17]): the water provides easy access to the foam and enables us to prepare precisely the chosen distribution of bubble areas. It also facilitates the manipulation of the boundaries, in particular that of the rubber bands (see below). The glass plate facilitates observation and prevents bubbles from breaking: the foam lifetime is limited only by coarsening, which takes several hours and does not affect the results presented below.

The trough is a rectangle 44 cm long and 20 cm wide. The foam is enclosed in a smaller square of size $18 \times 18 = 324 \, cm^2$, with four independent boundaries (Figure 1b). A rigid rod (fixed boundary) is attached to the trough itself. Another rigid rod (moving boundary) is attached to the glass lid, which slides laterally under the control of a motor. The rectangle is closed on each side by a rubber band (passive boundaries): it thus deforms into a parallelogram at constant area (Figure 2).

The trough is filled with a solution of 10% commercial dishwashing liquid in water. A pump blows air into a tube placed below the surface of water, which is moved back and forth to produce an homogeneous foam. At low flow rate, the solution surface tension and the tube diameter together fix the bubble volumes [18]. The histogram of bubble volumes therefore has a single peak. Its width increases with the flow rate, from 'narrow monomodal' (Figure 3a) to 'polydisperse' (Figure 3b). Using two tubes simultaneously yields a histogram of bubble volumes with two peaks. The distance between peaks can be chosen smaller than their width ('with shoulder', Figure 3c), or larger ('bimodal', Figure 3d).
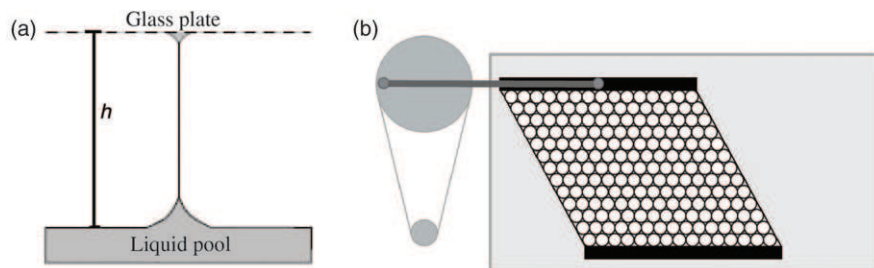

Figure 1. Experimental set-up. (a) Side view: bubbles are sandwiched between the water surface and a horizontal glass plate. (b) Top view: a computer controlled motor moves one rigid boundary, while the other one is fixed; the lateral boundaries are passive.

The shape of the bubbles, and thus the fraction of the glass plate touched by the water, varies with the foam thickness h [19], which is the distance between water and glass in the absence of bubbles (Figure 1a). At small h the foam is extremely wet and the bubbles are round. At large h the bubbles are dry but begin to pile on top of each other making a 3D foam [20]. We use the intermediate range ($3 < h < 6.8$ mm) for which the bubble monolayer is moderately wet. In this range, the bubbles can deform and store elastic energy. The foam has a finite shear modulus and thus behaves as a 2D elastic solid until it yields and bubbles rearrange.

2.2. *Measurements*

A circular fluorescent tube (diameter 48 cm) is placed just above the trough. A video camera records a 33 cm wide, 25 cm high field of view. Images are analysed using ImageJ (http://rsb.info.nih.gov/ij/) and skeletonised: white bubbles are surrounded by black boundaries with a thickness of one pixel. The number n of sides (i.e. of neighbours) of each bubble is measured without ambiguity. At a given h each bubble's volume determines its projected area seen from the top [21]. Hereafter we call 'bubble area' the area A of each skeletonised bubble. (In the original image, this corresponds to the area of the gas and almost all of the liquid.)

For each foam, we plot the histogram of A and n; Figure 3 shows different examples. We check that both averages, $\langle A \rangle$ and $\langle n \rangle$, have the expected values. Here the total number N of bubbles is typically 570–1800 (with a maximum of 2719); $\langle A \rangle$ is close to the total area of the foam divided by N (that is, the inverse of the bubble density), typically 18–65 mm^2; $\langle n \rangle$ is always equal to 6, minus a small correction of order $1/N$ [1,22].

We then measure the standard deviations $\Delta A = (\langle A^2 \rangle - \langle A \rangle^2)^{1/2}$ and $\Delta n = (\langle n^2 \rangle - \langle n \rangle^2)^{1/2}$. To enable comparisons, in what follows we only consider the dimensionless standard
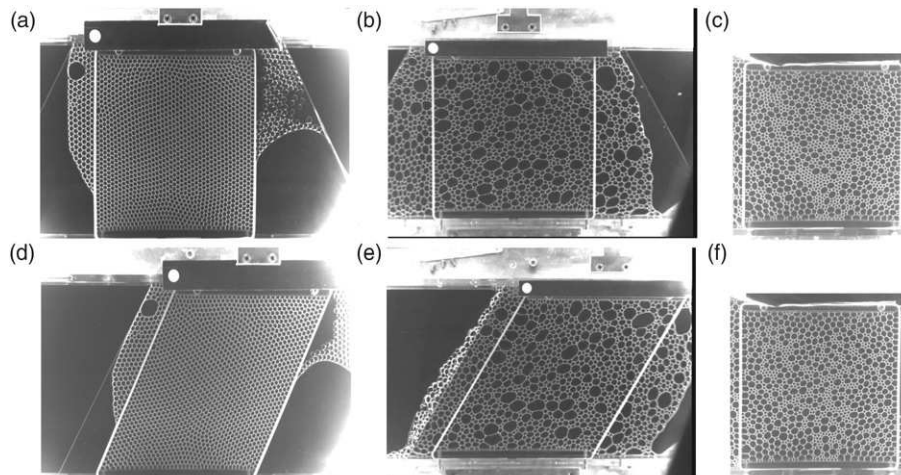

Figure 2. The foam is initially prepared within a square of side 18 cm (a,b,c) which can be deformed into a parallogram of the same area, here at an angle of 30° (d,e). The images show samples with the smallest (a,d) and largest (b,e) width $\Delta A / \langle A \rangle$ of the bubble area distribution. (f) Same bimodal foam as in (c), after 44 cycles of shear.
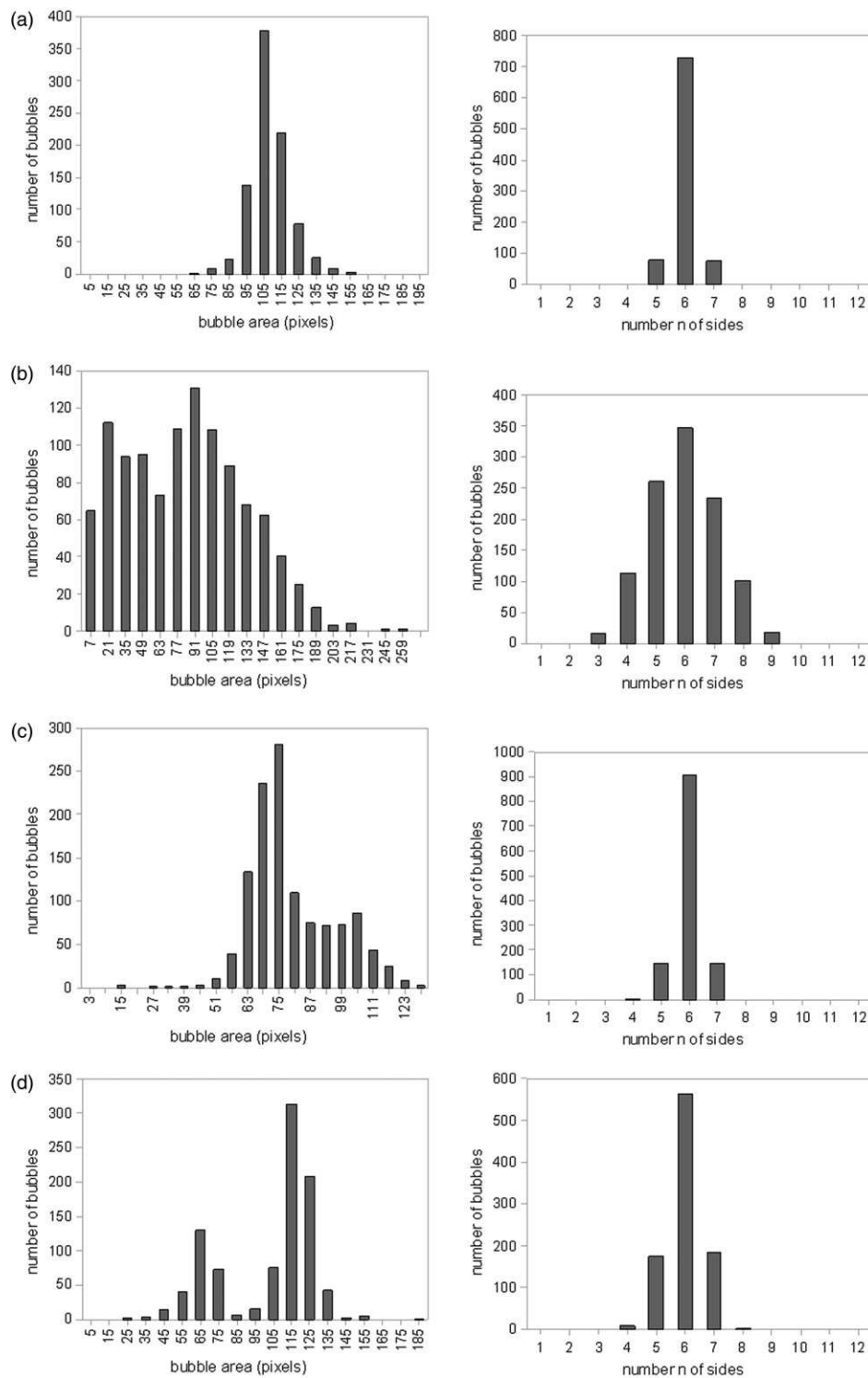
Figure 3. Four examples of histograms of bubble area *A* (left) and number *n* of sides (right) in freshly prepared foams: (a) narrow monomodal, (b) polydisperse, (c) with shoulder, (d) bimodal.

deviations $\Delta A/\langle A \rangle$ and $\Delta n/\langle n \rangle$ as measurements of the geometrical and topological disorders:

$$\frac{\Delta A}{\langle A \rangle} = \sqrt{\frac{\langle A^2 \rangle}{\langle A \rangle^2} - 1}; \quad \frac{\Delta n}{\langle n \rangle} = \sqrt{\frac{\langle n^2 \rangle}{\langle n \rangle^2} - 1}. \tag{1}$$

In principle, it is possible to define n unambiguously even for bubbles at the boundaries [5]. However, we choose to remove these bubbles (which may be poorly detected due to bias in the skeletonization) when evaluating both measures of disorder, which are very sensitive to changes in even a small number of bubbles [2].

2.3. *Shear cycles*

In agreement with theory [23] and simulations [24], all results presented below are independent of the strain amplitude if it is well above the yield strain. A shear cycle consists in shearing the foam by displacing the movable boundary a distance 10.4 cm and back, and then to -10.4 cm, and back again. This corresponds to an angle of $+30°$ to $-30°$ and a strain amplitude of $+10.4/18 = +0.58$ to -0.58. For dry foams, the yield strain is larger [23]; we obtain a larger strain amplitude by preparing the foam with the movable rod which is at the position -4.1 cm (at the left limit of the camera field of view): the cycle is then at positive strain from 0 to $(10.4 + 4.1)/18 = 0.8$, then down to $-(10.4 - 4.1)/18 = -0.35$. For the driest foam, we also reduce the size of the trough by reducing the distance between the fixed and movable rods to 10.5 cm; N is then smaller (413 versus 879 bubbles), and a cycle consists of positive strains in the range from 0 to $(10.4 + 4.1)/10.5 = 1.4$, then down to $-(10.4 - 4.1)/10.5 = -0.6$.

A cycle lasts for $T = 275$ s and the maximum velocity is $37.9°\ \text{min}^{-1}$, slow enough that the results presented here do not depend on the velocity. The bubble deformation and the velocity gradient enforced by the lateral boundaries are uniform (up to non-affine displacements due to local disorder). During shear, each cell area is conserved, so that $\Delta A/\langle A \rangle$ keeps its initial value. We measure $\Delta n/\langle n \rangle$ at each period.

3. Results

We cover a decade in $\Delta A/\langle A \rangle$, from about 0.1 to 1. Figure 2 shows foam samples with the smallest (Figure 2a and d) and largest (Figure 2b and e) width $\Delta A/\langle A \rangle$ of the bubble area distribution. We make the different kinds of distribution overlap, that is, the width of some polydisperse foams are larger than some bimodal foams. In principle, it would be possible to prepare foams for which the width of the area distribution is slightly larger than 1 by including a few very large bubbles. However, this would make the distribution spatially heterogeneous. At the other extreme, a foam with a width of the area distribution smaller than 0.1 would be possible with other experimental set-ups, but with only a small number of non-hexagonal bubbles the distribution of the number of sides would again become spatially heterogeneous.[2]

This range covers a large variety of foams already studied in the literature. Larger $\Delta n/\langle n \rangle$, up to 0.5 or 0.6, would instead correspond to simulated irregular-shaped structures

generated by fragmentation (fractal topological gas [25]). Lower $\Delta n/\langle n \rangle$, down to zero, can be obtained only in highly controlled structures, with periodic boundary conditions (as in simulations) or with boundaries far away from the analysed image. For instance, the fruit fly retina (Figure 6b) is part of a large honeycomb lattice of 800 facets.[3]

Figure 4 indicates a clear correlation between bubble size and number of sides for sheared foams (unsheared foams are similar, data not shown). There is still debate (for reviews see [1,2,6–14]) regarding (i) in which systems this relation is linear, following Lewis, or not linear; (ii) whether it is related to entropy maximisation, energy minimisation or both (free energy minimisation); (iii) what is the value and significance of the linear intercept; (iv) whether n correlates better with bubble perimeter or area (or volume, in 3D); (v) and especially up to what precision the relation can significantly be considered as linear for practical or theoretical applications. Here, in a narrow monomodal foam there are too few points to reach a conclusion; in polydisperse and bimodal foams the relation is certainly not linear, in agreement with references [13,14].

We usually perform measurements at an integer number of shear cycles (and, in some case, at half cycles). Any given pattern can be represented by a point in the plane $(\Delta A/\langle A \rangle, \Delta n/\langle n \rangle)$. During a shear experiment, this point moves vertically: the bubbles
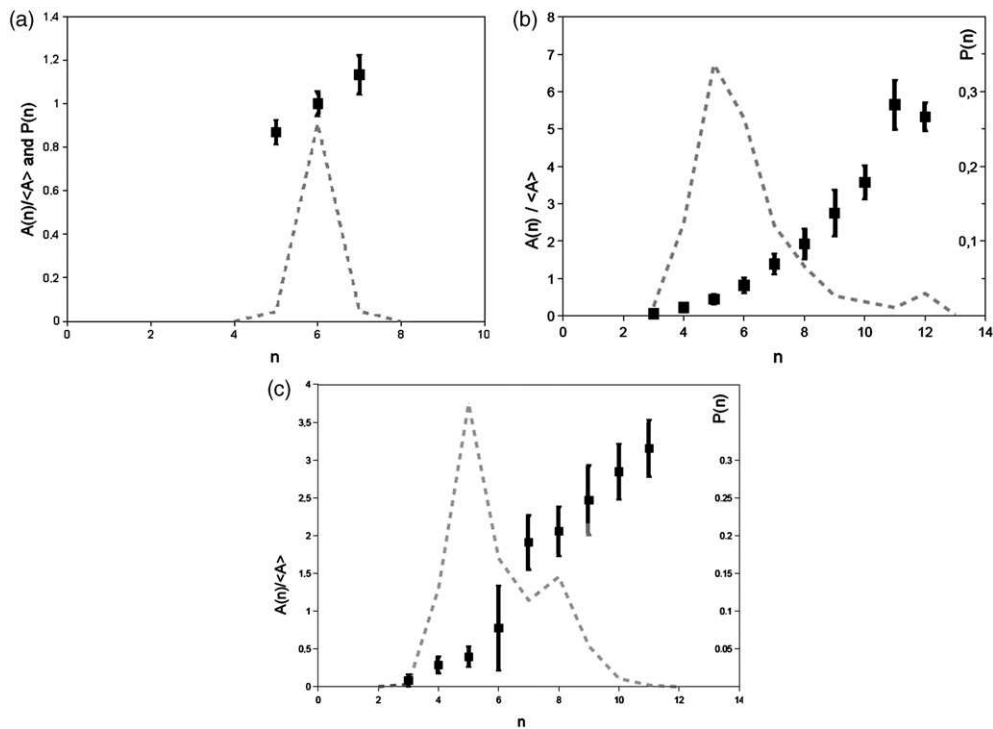

Figure 4. Size-topology correlation for foam experiments after several shear cycles: (a) narrow monomodal, (b) polydisperse, (c) bimodal. Closed squares: average size $\langle A(n) \rangle$ of the population of bubbles with n sides (made dimensionless by the global average area $\langle A \rangle$); bar: the standard deviation calculated on each population. Dashed line: proportion $P(n)$ of bubbles in this population.

rearrange and the distribution of the number of sides changes while the area distribution remains fixed. Weakly disordered foams become more ordered: $\Delta n/\langle n \rangle$ decreases. On the other hand, bimodal foams (Figure 2c and f) become increasingly mixed (Figure 5b): $\Delta n/\langle n \rangle$ increases. This is important and not trivial [4].
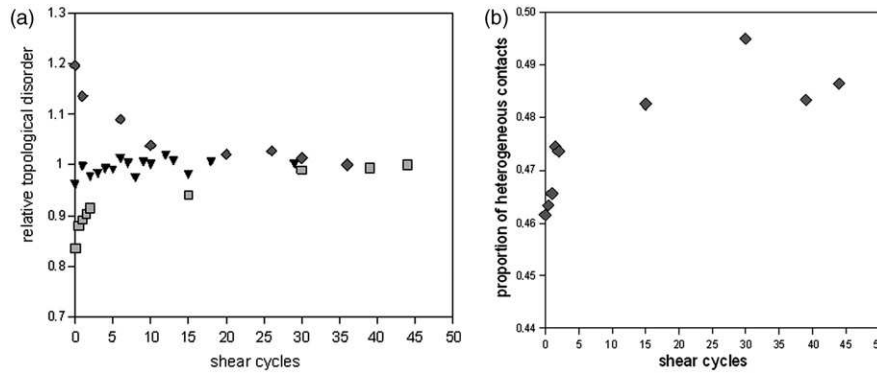

Figure 5. (a) Evolution of topological disorder under shear for given bubble area distribution – $\Delta n/\langle n \rangle$ (normalised by its asymptotic value to facilitate comparisons) versus number of shear cycles. Data correspond to Figure 4: diamonds – narrow monomodal; triangles – polydisperse; squares – bimodal. (b) Evolution of the fraction of contacts between unlike (small–large) bubbles during shear for a bimodal foam.
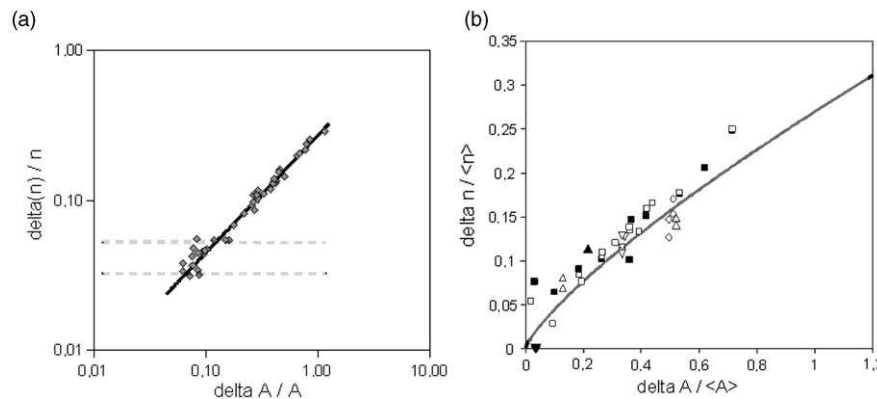

Figure 6. Correlation between measures of disorder. (a) *Sheared foams*: each point is the final value of $\Delta n/\langle n \rangle$ and $\Delta A/\langle A \rangle$. Solid line: power law $\Delta n/\langle n \rangle = 0.27(\Delta A/\langle A \rangle)^{0.8}$. Dashed lines: lower bound for topological disorder (See note 2) [26], for the extreme values of N in these experiments (413 and 2719). Note the log–log scale. (b) *Other systems*: Solid line: Equation (2), same as in (a). *Open symbols*: *foam simulations*; open downward-pointing triangles, Surface Evolver [27] simulations [23] shuffled by cycles of shear, as in the present experiments; open upward-pointing triangles, same with periodic boundary conditions [23]; open diamonds, Surface Evolver simulations shuffled by cycles of uniaxial elongation [24]; open squares, Potts model simulations at constant tension, with periodic boundary conditions, shuffled by increasing the fluctuations [28,30]. *Closed symbols: biological cells*; closed downward-pointing triangles, facets (ommatidia) in a fruit fly (Drosophila) retina are arranged in an ordered honeycomb; closed upward-pointing triangles, same for the *rough eye* mutant retina [29]; closed square, simulations using the Potts model of cells with adhesion and cortical tension, with periodic boundary conditions, shuffled by increasing the fluctuations [28,30].

In all experiments, $\Delta n/\langle n \rangle$ reaches a plateau after a few shear cycles (Figure 5a). Final values tend to cluster on a single curve (Figure 6a), namely, the power law:

$$\frac{\Delta n}{\langle n \rangle} = 0.27 \left(\frac{\Delta A}{\langle A \rangle} \right)^{0.8}. \tag{2}$$

This is the main result of this article. It does not seem to depend on the distribution's shape (higher moments). In our foams, the width of the area distribution varies from 0.1 to 1, and that of the topology distribution from 0.03 to 0.3. In this limited range, Equation (2) means that $\Delta n/\langle n \rangle$ is close to $0.3 \, \Delta A/\langle A \rangle$.

4. Discussion

According to de Almeida and coworkers [31–33], 'shuffling' a foam involves enough topological changes ('T1' neighbour swappings, considered here ; or 'T2' cell disappearance during coarsening [1]) that it loses any memory of its initial condition. The present results make this definition precise: a foam is shuffled after enough rearrangements [23] that the topological disorder becomes more dependent on the geometrical disorder than on the initial conditions.

This statistical (rather than exact) correlation of Equation (2) is not trivial. The curve of Figure 6a seems to be stable under shuffling: it is reached asymptotically, when starting from different initial conditions (Figure 5). It does not seem related to the minimisation of any energy, and could apply to other systems. Examples from foam simulations as well as biological tissues are plotted on Figure 6b. The collected data all fall in the same region of the (*geometrical disorder*, *topological disorder*) plane. Most of them have $\Delta n/\langle n \rangle$ larger (up to 1.5 or 2 times) than Equation (2).

The curve of Figure 6a appears as a statistical (rather than exact (See note 1), see the case of non-shuffled foam in Figure 5b) lower bound for the topological disorder, at given area disorder. It can be used in practice as a benchmark to test how shuffled a pattern is. If a pattern has $\Delta n/\langle n \rangle$ very different from $0.3\Delta A/\langle A \rangle$, it probably means that it is far from being shuffled. There is no reciprocity: a non-shuffled pattern can be close to Equation (2).

5. Conclusion

To summarize, all the patterns that we examine are in the same region of the plane (*geometrical disorder*, *topological disorder*). For a given width of the area distribution (and independently of its higher moments), the 'shuffled foam' is well defined and realised. It reaches a lower bound (Equation (2)) for the topological disorder, which is robust and directly dependent on the geometrical disorder: $\Delta n/\langle n \rangle$ is close to $0.3\Delta A/\langle A \rangle$. Theoretical work could try to explain Equation (2) and its stability, for instance, by understanding the respective roles of disorder and surface minimisation [31–33].

These results could be used to characterise patterns and determine causal relations between both disorders. They could also be used to study how the foam's disorder (now quantified by a single number) affects its mechanical properties [24], and to improve the characterisation of coarsening [3,33]. Perspectives include the study of fluctuations of $\Delta n/\langle n \rangle$, for example, within a shear cycle, and the generalisation of Equation (2) to other

discrete systems, such as granular matter and colloids [34,35], biological tissues [36] and 3D systems [33].

Notes

1. For any $\Delta A/\langle A \rangle$ it would be possible to construct a (non-shuffled!) foam of arbitrarily small $\Delta n/\langle n \rangle$, as in [4]. Consider a bimodal foam, where small bubbles, arranged in a honeycomb, would be surrounded by a honeycomb of large bubbles. Non-hexagonal bubble would be at the boundary between both honeycombs, and thus of order $\sqrt{N}$. Thus by increasing N, $\Delta n/\langle n \rangle$ could be made arbitrarily small.
2. When enclosing a honeycomb in a square box, boundary conditions impose at least two grain boundaries with length of order $N^{1/2}$ between perpendicular lattices. Topological considerations [26] imply a minimal number of paired five- and seven-sided bubbles per unit line of grain boundaries. We then estimate the topological disorder to be at least $1/[3 \times 12^{1/8} \times N^{1/4}]$.
3. Note that the topological order is already present before the retina is entirely differentiated and the facet area can be defined: see Figure 2G, H of F. Chanut *et al.*, Genetics 160 (2002) 623.

References

[1] D. Weaire and N. Rivier, Contemp. Phys. 25 (1984) p.5.
[2] J.A. Glazier, Dynamics of cellular patterns, PhD thesis, University of Chicago, Chicago, 1989.
[3] J.A. Glazier and D. Weaire, J. Phys.: Condens. Matter 4 (1992) p.1867.
[4] P.I.C. Teixeira, F. Graner and M.A. Fortes, Eur. Phys. J. E 9 (2002) p.161.
[5] F. Graner, Y. Jiang, E. Janiaud et al., Phys. Rev. E 63 (2001) p.011402.
[6] F.T. Lewis, Anat. Records 38 (1928) p.341; 50 (1928) p.235.
[7] C.S. Smith, *Metal Interfaces*, American Society for Metals, Cleveland, 1952, p.65.
[8] N. Rivier and A. Lissowski, J. Phys. A: Math. Gen. 15 (1982) p.L143.
[9] P. Pina and M.A. Fortes, J. Phys. D 29 (1996) p.2507.
[10] N. Rivier, *Statistical thermodynamics of foams*, in *Foams and Emulsions*, J.J. Sadoc and N. Rivier, eds., Kluwer, Boston, 1999, p.105.
[11] N. Rivier, *Disorder and Granular Media*, D. Bideau and A. Hansen, eds., Elsevier, New York, 1993, p.55.
[12] M.A. Fortes and P.I.C. Teixeira, J. Phys. A: Math. Gen. 36 (2003) p.5161.
[13] C. Annic, J.-P. Troadec, A. Gervois et al., J. de Phys. I France 4 (1994) p.115.
[14] V. Parfait-Pignol, G. Le Caër and R. Delannay, Eur. Phys. J. B 4 (1998) p.499.
[15] A. Abd el Kader and J.C. Earnshaw, Phys. Rev. Lett. 82 (1999) p.2610.
[16] M.F. Vaz and M.A. Fortes, J. Phys. Cond. Matter 9 (1997) p.8921.
[17] M.F. Vaz and S.J. Cox, Philos. Mag. Lett. 85 (2005) p.415.

[18] R. Clift, J.R. Grace and M.E. Weber, *Bubbles, Drops and Particles*, Academic Press, New York, 1978.
[19] B. Dollet and F. Graner, J. Fluid Mech. 585 (2007) p.181.
[20] S.J. Cox, D. Weaire and M.F. Vaz, Euro. Phys. J. E 7 (2002) p.311.
[21] C. Raufaste, B. Dollet, S. Cox et al., Eur. Phys. J. E 23 (2007) p.217.
[22] W.C. Graustein, Ann. Math. 32 (1931) p.149.
[23] C. Raufaste, Rhéologie et imagerie des écoulements 2D de mousse. PhD thesis University of Grenoble (2007). Available at: http://tel.archives-ouvertes.fr/tel-00193248/fr/
[24] S.J. Cox, J. Non-Newtonian Fl. Mech. 137 (2006) p.39.
[25] R. Delannay and G. Le Caër, Phys. Rev. Lett. 73 (1994) p.1553.
[26] L. Alfonso, M.E. Rosa and M.A. Fortes, Coll. Surf. A 309 (2007) p.38.
[27] K. Brakke, Exp. Math. 1 (1992) p.141.
[28] A.F.M. Marée, V.A. Grieneisen and P. Hogeweg, *The cellular Potts model and biophysical properties of cells, tissues and morphogenesis*, in *Single Cell Based Models in Biology and Medicine*, A.R.A. Anderson, M.A.J. Chaplain and K.A. Rejniak, eds., Birkhäuser-Verlag, Basel, 2007, p.107.
[29] T. Hayashi and R.W. Carthew, Nature 431 (2004) p.647.
[30] J. Käfer, T. Hayashi, A.F.M. Marée et al., Proc. Nat. Acad. Sci. USA 104 (2007) p.18549.
[31] R.M.C. de Almeida and J.R. Iglesias, J. Phys. A 21 (1988) p.3365; J.R. Iglesias and R.M.C. de Almeida, Phys. Rev. 43 (1991) p.2763.
[32] R.M.C. de Almeida and J.C.M. Mombach, Physica A 236 (1997) p.268.
[33] G.L. Thomas, R.M.C. de Almeida and F. Graner, Phys. Rev. E 74 (2006) p.021407.
[34] P. Ziherl and R.D. Kamien, J. Phys. Chem. B 105 (2001) p.10147.
[35] C.N. Likos and C.L. Henley, Philos. Mag. B 68 (1993) p.85.
[36] S. Courty, J. Friedlander, F. Graner et al., preprint (2008).